Proceedings of the 1996 IEEE
International Conference on Robotics and Automation
Minneapolis, Minnesota - April 1996

Adaptive Gait Control of a Biped Robot based on Realtime Sensing of the Ground Profile

Shuuji Kajita* and Kazuo Tani

Mechanical Engineering Laboratory
Namiki 1-2, Tsukuba, Ibaraki 305 JAPAN
* E-mail kajita@mel.go.jp

Abstract

In this paper, realtime control of dynamic biped locomotion using sensor information is investigated. We used an ultrasonic range sensor mounted on the robot to measure the distance from the robot to the ground surface. During the walking control, the sensor data is converted into a simple representation of the ground profile in realtime. We also developed a control architecture based on the Linear Inverted Pendulum Mode which we proposed previously for dynamic walking control. Combining the sensory system and the control system enabled our biped robot, Meltran II, to walk over ground of unknown profile successfully.

1 Introduction

One of the most important advantages of legged robots is the ability to move over rough terrain. Many quadrupeds and hexapods for walking on rough terrain have been developed [4, 8, 11], but not so many bipeds, because a biped robot must not only deal with ground unevenness but also maintain dynamic stability.

Hodgins and Raibert studied the control of a biped running on rough terrain. Based on Raibert's hopping control algorithm [10], they investigated the method of controlling the length of steps so that the feet land on the available footholds, and demonstrated a biped running up and down stairs [5].

Zheng, et al. achieved control of static biped locomotion on an unknown sloping surface using position sensors on the joints and force sensors underneath the heel and toe [17]. Oh-hata, et al. carried out experiments on a dynamic biped walking on stairs by measuring the shape of the stairs with a range finder and adjusting the footholds [16]. Yamaguchi, et al. developed a special foot mechanism with shock absorbing material and sensor system for ground unevenness [13]. Using this mechanism they developed a biped walking control which adapts to an unknown uneven surface [14].

In most of the above studies, the control systems generate walking motions by modifying the nominal walking pattern which are dynamically or statically stable, therefore the walking pattern does not change drastically. But, when a biped robot changes its gait to suit the ground, it can traverse more difficult terrain. This paper discusses the adaptive gait control method of a biped robot by realtime sensing of the ground profile. For this purpose, we propose a control method based on the linear inverted pendulum mode which we have proposed previously for a dynamic biped walking on rough terrain [6, 7].

2 Ground profile

In this paper, we adopted an ultrasonic range sensor for measuring the ground profile. It is difficult to detect sloping surfaces by such sensors, so we limit the descriptions in this paper to walking on ground constituted by planes and vertical steps, such as stairs or platforms. Yoneda called such terrain "Horizontally Composed (HC)," and discussed the mechanism and control of a biped robot on such ground [15, 16].

3 Experimental apparatus

Figure 1 shows our biped robot "Meltran II" used for the experiments. Meltran II is a six D.O.F. biped robot of height approximately 40 cm and weight 4.7 kg. Each leg consists of a parallel link driven by two DC servomotors with reduction gears (11 W, reduction ratio: 1/69.3) installed on the body. Each ankle is driven by a servomotor (6.4 W, reduction ratio: 1/34.7) mounted near the knee. We adopted such a design to lighten the legs. As a result, the center of mass of the whole robot is always near the hip joint.

To keep static stability in the lateral directions, the robot has wide feet extending toward inside, thereby restricting the walking motion to a sagittal plane.

Using a personal computer [PC9801BA, i486DX (66 MHz)] and DSP [μPD77230 (6.7 MHz)], we applied local position feedback to each joint of the legs and controlled the body motion as shown in the next section. The servo cycle was 1 ms.

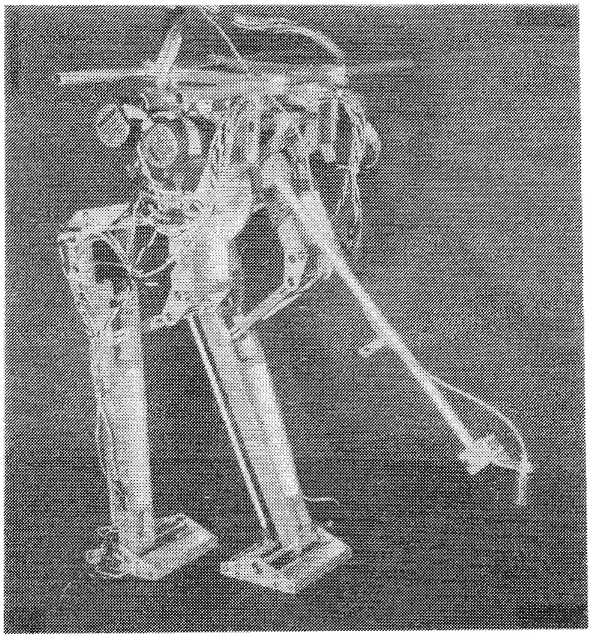

Figure 1: Biped robot "Meltran II"

To obtain information on the ground profile, a sensor head (Keyence, UD-1130) was mounted on the tip of a pipe extending forward from the robot body. Using this sensor, the robot can measure the height of the point 30 cm ahead of the hip joint.

4 Control on a rugged terrain

This section explains the control based on the linear inverted pendulum mode. To simplify the explanation, we assume that the center of mass of the whole robot is exactly on the hip joint. For detailed control, see [7].

(a) Setting constraint line

Figure 2 shows the one step motion with the point P_2 as the current foothold. In this figure, the robot is represented by two lines connecting the hip joint (= the center of mass of the robot) to the foothold point, and to the tip of the swing leg. P_1 and P_3 are footholds of one step before and one step after, respectively. Q_1, Q_2 and Q_3 are the points at the same height y_c above the foothold points. R is the point where the swing leg passes, and is set at an adequate height above P_2.

For the explanation, we divide the support period at the time when the center of mass passes Q_2, and call the periods before that moment and after that moment the 'first half of the support' and the 'latter half of the support', respectively. The robot is controlled in each period as follows:

First half of the support: The center of mass is controlled to move on the line $\overline{Q_1Q_2}$ using the joint torques of the support leg. The slope of the constraint line is,

$$k_1 = \frac{y_2 - y_1}{x_2 - x_1}.$$

The tip of the swing leg moves from P_1 to R.

Latter half of the support: The center of mass is controlled to move on the line $\overline{Q_2Q_3}$ using the joint torques of the support leg. The slope of the constraint line is,

$$k_2 = \frac{y_3 - y_2}{x_3 - x_2}.$$

The tip of the swing leg moves from R to P_3.

where $(x_1, y_1), (x_2, y_2), (x_3, y_3)$ are the coordinates of the footholds of P_1, P_2, P_3, respectively.

The constraint line $\overline{Q_1Q_2}$ in the first half of the support is also used in the latter half of one step before (foothold: P_1). This means that the slope k_1 of the constraint line has already been calculated at the beginning of the current support. The slope k_2 for the latter half of the support must be calculated by the time the center of mass passes the point Q_2. Thus, the coordinates of the next foothold Q_3 are required for this calculation. k_2 is used in the first half of the support of one step after (foothold: P_3). In this way, the slope for each step is calculated from the position of the next foothold whose height is determined according to the ground profile.

(b) Control of horizontal motion of the body

When the center of mass of the robot is controlled on a constraint line like Fig.2, the horizontal dynamics of the center of mass of the body can be represented approximately by the following simple equation [6].

$$\ddot{x} = \frac{g}{y_c}x + \frac{1}{my_c}u_1 \quad (1)$$

where x is the horizontal displacement of the center of mass from the current foothold, m is the mass of the robot, and u_1 is the ankle torque of the support leg.

To guarantee predictable motion of the robot, the ankle torque u_1 is controlled as follows:

$$u_1 = k_P(x_{ref} - x) + k_D(\dot{x}_{ref} - \dot{x}) + k_I \sum (x_{ref} - x)\Delta t \quad (2)$$

where

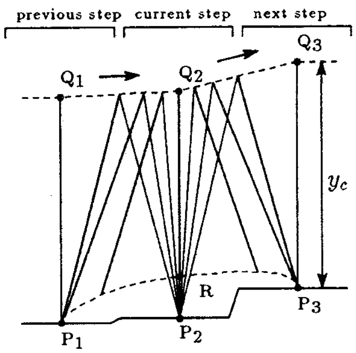

Figure 2: Motion planning on rugged terrain

Δt: sampling time (1ms)
k_P, k_D, k_I: feedback gains

$x_{ref}, \dot{x}_{ref}$ are the reference position and velocity generated by following equation.

$$\ddot{x}_{ref} = \frac{g}{y_c} x_{ref} \quad (3)$$

By such control, the horizontal motion of the center of mass follows eq.(3) even if there are disturbances or parameter errors in the mechanism.

(c) Control of gait and swing leg

The motion in accordance with eq.(3) can be classified into four basic patterns (Fig.3). To represent the motion patterns uniformly, the state when the speed becomes zero is used in patterns I and III, and the state when x becomes zero is used in patterns II and IV. Such states are marked with a black circle in Fig.3 and we describe them as $(\bar{x}, \bar{v})$ [1]. Table 1 shows the relationship between the four patterns, $(\bar{x}, \bar{v})$, and the corresponding walking motion. The support phase motion of each step is determined by the condition of the support leg exchange (Fig.4). We assume that the support leg is exchanged instantaneously, and that the velocity of the center of mass does not change at this time. When the motion of the support phase at P_1 is $(\bar{x}_1, \bar{v}_1)$ and the motion of the support phase at P_2 is $(\bar{x}_2, \bar{v}_2)$, the horizontal position x_f and horizontal speed v_f at the moment of the exchange are given by the following equations [6]:

Table 1: Characteristics of four basic patterns

Pattern	Parameters	Corresponding motion
I	$\bar{x} > 0, \bar{v} = 0$	walk start/end, stepping
II	$\bar{x} = 0, \bar{v} > 0$	walk forward
III	$\bar{x} < 0, \bar{v} = 0$	walk start/end, stepping
IV	$\bar{x} = 0, \bar{v} < 0$	walk backward

[1] In this definition, one element of $(\bar{x}, \bar{v})$ becomes zero. We use them as a pair to represent the four types of movements uniformly.

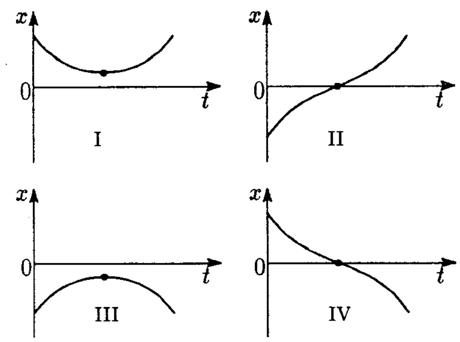

Figure 3: Four basic patterns of support phase motion

$$x_f = \frac{y_c}{gs}(E_2 - E_1) + \frac{s}{2} \quad (4)$$

$$v_f = \sqrt{2E_1 + \frac{g}{y_c} x_f^2} \quad (5)$$

$$E_1 \equiv -\frac{g}{2y_c}\bar{x}_1^2 + \frac{\bar{v}_1^2}{2}$$

$$E_2 \equiv -\frac{g}{2y_c}\bar{x}_2^2 + \frac{\bar{v}_2^2}{2}$$

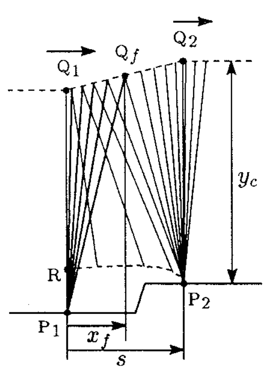

Figure 4: Support exchange

To achieve this support leg exchange, the tip of the swing leg must be controlled to land on the next foothold P_2 at the time the support leg is exchanged. The time τ required for the center of mass to move from Q_1 to Q_f is easily calculated from the analytical solution of eq.(3):

$$\tau = T_c \ln\left(\frac{x_f + T_c v_f}{\bar{x}_1 + T_c \bar{v}_1}\right) \qquad (6)$$

where $T_c = \sqrt{y_c/g}$. The trajectory of the swing leg is designed so as to take time τ to move from R to P_2. Control on the support leg and swing leg is switched the instant of the swing leg lands.

5 Sensor data processing

5.1 Map of the ground profile

This section explains the data processing for preparing a map of the ground profile based on the information of the ultrasonic sensor mounted on the robot. Figure 5 shows the positional relationship between the sensor mounted on the robot and the ground profile (the thickness of the feet is neglected here). The sensor head axially emits an ultrasonic beam focused to 2 mm diameter for measuring the distance to an object with a resolution of 0.3 mm. Inclination of the reflecting surface is allowed up to ±9 degrees (nominal performance). From the sensor only the distance y_{sens} to the ground is obtained directly. But, combining this with the joint angles of the support leg at the same time, the robot can specify a point (detection point) on the ground with reference to the current foothold.

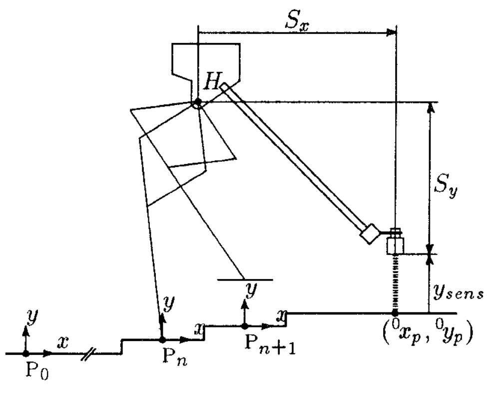

Figure 5: Robot and ultrasonic sensor

$$\begin{aligned} {}^n x_p &= x_h + S_x - (S_y + y_{sens})\theta_{body} &(7)\\ {}^n y_p &= y_h - y_{sens} - S_y - S_x\theta_{body} &(8)\end{aligned}$$

where

$({}^n x_p, {}^n y_p)$: coordinates of a point on the ground with the n-th foothold P_n regarded as the origin

(x_h, y_h): position of joint H with the foothold regarded as the origin

(S_x, S_y): position of sensor head from the hip joint

θ_{body}: inclination of the body from the vertical (clockwise +)

The third term of the right side of eq.(7) considers the deflection of the ultrasonic beam due to body rotation. The fourth term of the right side of eq.(8) compensates for the vertical motion of the sensor head due to body rotation. These were necessary because the robot body was deflecting about ±1 degree from the vertical due to control errors, although it was controlled to be vertical constantly.

The ground profile relative to the current foothold is converted into an absolute coordinate whose origin is the first foothold P_0 at the start of walking. A sensed position in the absolute coordinate $({}^0x_p, {}^0y_p)$ is given by the following equations.

$$\begin{aligned} {}^0 x_p &= {}^0 x_n + {}^n x_p &(9)\\ {}^0 y_p &= {}^0 y_n + {}^n y_p &(10)\end{aligned}$$

where $({}^0x_n, {}^0y_n)$ is the position of each foothold in the absolute coordinate. We can easily calculate this by adding the step length and height difference.

In the experiments, we made the above calculation every 10 ms, storing the results in an array as a map of the ground profile. By scanning the data, the walking control system can know the height of the ground at any position which has been already scanned by the sensor.

5.2 Landing area map

The landing area map is a 1D map of the safe footholds where the robot can put its foot. This 1D map is calculated from the 2D map of the ground profile captured as described in the last section.

Because the ground profile considered in this paper is HC terrain constituted by a horizontal plane and vertical steps, the only place that the robot can not land is a vertical step. The existence of a vertical step can be detected from the following equation.

$$dy[i] = ({}^0y_p[i] + {}^0y_p[i-1] - {}^0y_p[i-2] - {}^0y_p[i-3])/4 \qquad (11)$$

where ${}^0y_p[i]$ is the height of the ground obtained every 10 ms. When the absolute value of $dy[i]$ exceeds a threshold, we regard that a step has been detected, and set the following range as the landing-inhibited area to prevent the robot from landing on the edge of a step.

$${}^0x_p[i] - d < x < {}^0x_p[i] + d \qquad (12)$$

where d is half the length of the foot of Meltran II (feet are symmetrical, $d = 4$ cm).

The landing area map is obtained by sequentially excluding the landing-inhibited area from the area scanned by the ultrasonic sensor. Because the coordinate data of the ground profile are obtained every 10 ms during walking, the landing area map is updated simultaneously.

Figure 6 shows data of the ground profile, $dy[i]$, and the landing area map (thick line segments with circles on the ends) obtained from such data.

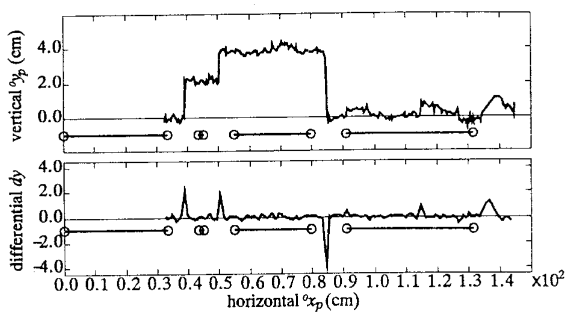

Figure 6: Landing area map

The landing area map is also represented by the set M shown below.

$$\mathsf{M} \equiv \{[m_{s1}, m_{e1}], [m_{s2}, m_{e2}] \cdots\}$$

where m_{si}, m_{ei} $(i = 1, 2 \ldots)$ are the start and end points of each landing area.

6 Gait control

6.1 Safe walking conditions and stepping gait

Let us discuss how much information on the ground profile a biped robot should know. As a specific example, we consider the situation in which a robot approaches a ditch as shown in Fig.7.

Let us assume that the robot has stepped on P_1 and P_2, but could not find the next foothold P_3 due to the ditch. If the support phase motion at P_2 is type II (see Fig.3), the robot can not avoid falling into the ditch. So the support phase motion at P_2 must be changed from type II to type III. This is determined by the exchange of support leg at Q_f. Furthermore, the movement RP_2 of the swing leg to achieve this exchange is calculated just before the center of mass passes Q_1 (see section 4). Thus, the robot cannot stop safely unless it finds that the foothold P_3 does not exist before the center of mass passes Q_1. This can be summarized as follows:

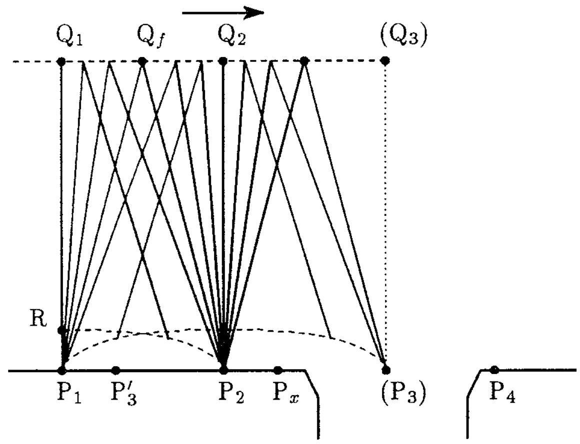

Figure 7: Stopping for a ditch

Safe walking condition: To continue safe walking, footholds of two steps ahead must always exist.

In Fig.7, the robot can stride over the ditch if it lands on P_x and uses the maximum step length from there. However, it can happen that P_2P_x is too short for the step length and P_1P_x is too long, due to the adjustable limit of the step length as explained in the next section. In such a case, the next foothold of P_2 should be at P'_3, and the robot should tread on P_x as the third step. In this case, the center of mass draws a trajectory as shown in Fig.8. We call such a gait to adjust a foothold the "stepping gait."

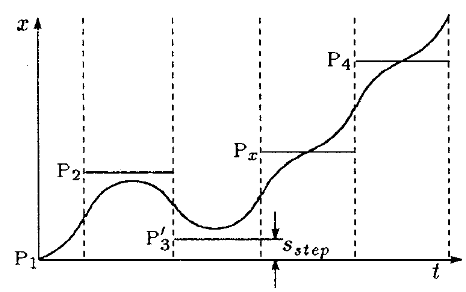

Figure 8: Stepping gait

6.2 Step length variable range

Before formulating the foothold selection algorithm, we must determine the nominal ranges of step length. The maximum step length s_{max} of Meltran II is determined by the mechanical limit of the legs. Having feet which restrict walking to a sagittal plane, Meltran II cannot have a step length of less than 8 cm. We determined the minimum step length ($s_{min} = 10$ cm) by adding a safety margin to this.

In addition, we have also determined the default (standard) step length s_d, and standard stepping gait pitch s_{step} (see Fig.8). The parameters used in the experiments are listed in Table 2.

Table 2: Parameters for step length control

Maximum step length	s_{max}	16.0 cm
Minimum step length	s_{min}	10.0 cm
Default step length	s_d	12.0 cm
Stepping gait pitch	s_{step}	2.0 cm

6.3 Foothold selection algorithm

The foothold selection algorithm calculates the footholds one and two steps ahead (P_1, P_2) from the current foothold (P) and the landing area map (M) considering safe walking conditions. If a foothold two steps ahead can not be found, the foothold for the stepping gait is calculated. We used the following algorithm (see Fig.9).

(1) Calculate S_1, the landing area of one step ahead, as the product of M and the reachable area from P.

(2) Calculate S_2, the landing area of two steps ahead, as the product of M and the reachable area from S_1. If S_2 does not exist go to (2)'.

(3) Select the foothold P_2 as the closest point to $2s_d$ in S_2.

(4) Calculate S'_1, the landing area, as the product of S_1 and the reachable area backward from P_2.

(5) Select the foothold P_1 as the closest point to s_d in S'_1. (END)

(2)' (If a foothold two steps ahead does not exist): Calculate S_3 as the product of M and the reachable area backward from S_1.

(3)' Select the foothold P_2 as the closest point to s_{step} in S_3.

(4)' Calculate S'_1 as the product of S_1 and the reachable area from P_2.

(5)' Select the foothold P_1 as the closest point to s_d in S'_1. (END)

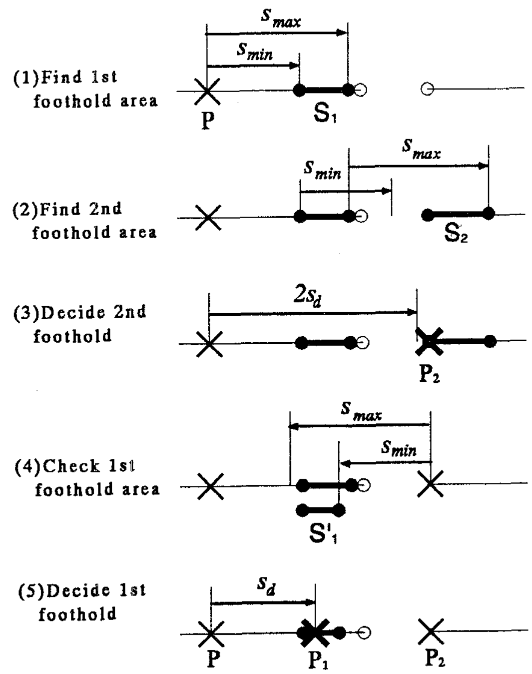

Figure 9: Obtaining footholds of two steps

From the above algorithm we can calculate the step length of one step ahead s_1 and the step length of two steps ahead s_2. A negative s_2 means transfer to the stepping gait. Generally, the motion pattern of the next support phase is determined by the current pattern and the sign of s_2, i.e. the direction of two steps ahead. Figure 10 shows the transition of the motion pattern of the support leg phase.

For example, the transition II→III→IV means the transfer from forward walking to backward walking. The transition I→III→I→III means marking time. By tracing the arrows shown in Fig.10, we can obtain all possible gaits which can be realized by the biped robot in a sagittal plane.

7 Results of experiment

We carried out an experiment on ascending and descending simple stairs of plywood, having two 1.9 cm up steps and one 3.8 cm down steps. The stairs were placed on an iron plate and coated with 2 mm thick rubber sheet to prevent the robot from slipping.

Figure 11 shows the results of the experiment as a stick picture. In the experiment, the robot used the stepping gait twice to adjust the foothold on the stairs.

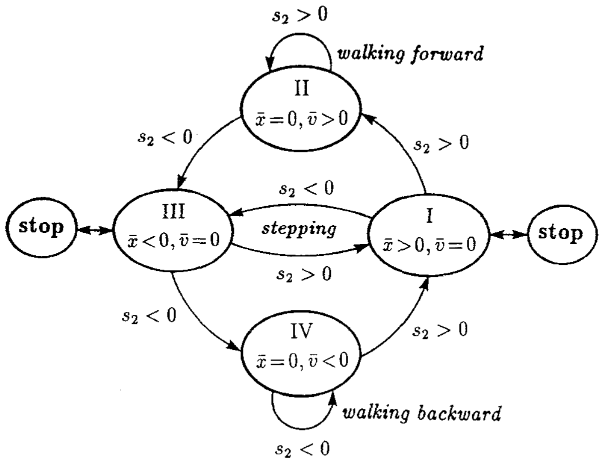

Figure 10: State transition of support phase

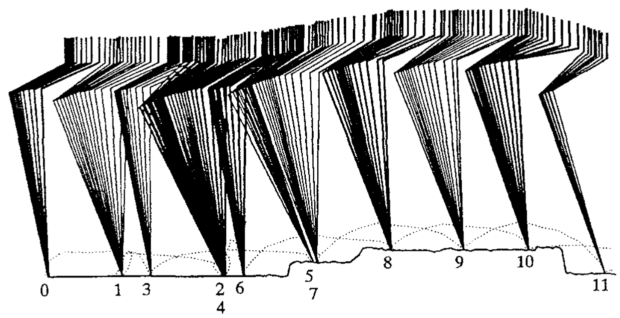

Figure 11: Experimental result (stick picture)

The number at each foothold indicates the sequence of landing.

Figure 12 shows the horizontal motion of the feet during the same experiment. The two curved lines show the horizontal displacement of the right and left feet from the hip joint.

The vertical broken lines show the touchdown timing of the swing leg and the beginning of the new support phase. In the experiments, we exchanged the support leg via dual leg support, though we explained the control based on instantaneous exchange of the support leg in section 4. The dual leg support period effectively reduced the impact force at exchanges and increased the success ratio of the walking experiment. The robot was supported by both legs about 15% of the time, but this causes no substantial change to the control algorithm.

The wider spaces between the vertical broken lines mean the periods of single leg support. Figure shows the types of patterns used at each support phase by I, II, and III.

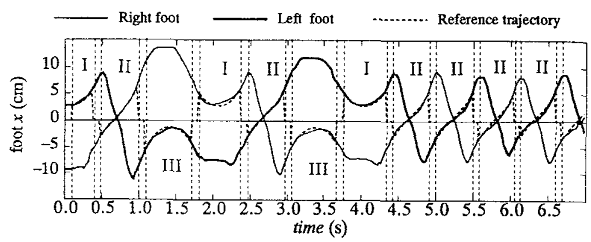

Figure 12: Experimental result (horizontal motion)

8 Conclusion

This paper discussed an adaptive gait control of a biped robot based on realtime sensing of the ground profile. Using the linear inverted pendulum mode, we could easily construct a walking control system which can adapt to unknown ground.

Since we used an ultrasonic sensor to obtain the ground profile, discussions and experiments in this paper were limited to walking on the terrain constituted by horizontal planes and vertical steps without slopes. However, if the sensor system is improved, our method can be expanded for ground of various profiles, and we shall address this issue in future work.

References

[1] Alexander, R.M, "Gaits of mammals and turtles," Journal of the Robotics Society of Japan, Vol.11, No.3, pp.314-319, 1993.

[2] Furusho, J. and Masubuchi, M., "A Theoretically Motivated Reduced Order Model for the Control of Dynamic Biped Locomotion," ASME Journal of Dynamic Systems, Measurement, and Control, Vol.109, 1987, pp.155-163

[3] Gubina, F., Hemami, H., and McGhee, R.B., "On the Dynamic Stability of Biped Locomotion," IEEE Trans. on Biomedical Engineering, BME-21-2, 1974, pp.102-108

[4] Hirose, S., Yoneda, K., et al., "Design of Prismatic Quadruped Walking Vehicle TITAN VI," Proceedings of the 5th International Conference on Advanced Robotics, 1991, pp.723-738

[5] Hodgins, J.K. and Raibert, M.H., "Adjusting step length for rough terrain locomotion," IEEE Trans. on Robotics and Automation, Vol.7, No.3, 1991, pp.289-298

[6] Kajita, S. and Tani, K., "Study of Dynamic Biped Locomotion on Rugged Terrain," Proceedings of the 1991 IEEE International Conference on R & A, 1991, pp.1405-1411

[7] Kajita, S. and Tani, K., "Experimental study of biped dynamic walking in the linear inverted pendulum mode," Proceedings of the 1995 IEEE International Conference on R & A, 1995, pp.2885-2891

[8] Nagy, P.V., Whittaker, W.L. and Desa, S. "A Walking Prescription for Statically-Stable Walkers Based on Walker/Terrain Interaction," Proceedings of the 1992 IEEE International Conference on R & A, 1992, pp.149-156

[9] Mulder, M.C., Shaw, J., and Wagner, N., "Adaptive Control Strategies for a Biped," ASME, Robotics Research — 1989, DSC-Vol.14, 1989, pp.113-117

[10] Raibert, M.H., "Legged robots that balance," MIT Press:Cambridge, 1986

[11] Song, S.M. and Waldron, K.J., "Machines that Walk; The Adaptive Suspension Vehicle," MIT Press, 1989

[12] Takanishi, A., Ishida, M., Yamazaki, Y., and Kato, I., "The Realization of Dynamic Walking by the Biped Walking Robot WL-10RD," Proceedings of '85 International Conference on Advanced Robotics (ICAR), 1985, pp.459-466

[13] Yamaguchi, J., Takanishi, A., and Kato, I., "Experimental development of a foot mechanism with shock absorbing material for acquisition of landing surface position information and stabilization of dynamic biped walking," Proceedings of the 1995 IEEE International Conference on R & A, 1995, pp.2892-2899

[14] Yamaguchi, J., et al., "Dynamic biped walking adapting to an unknown uneven surface by a biped walking robot having a foot mechanism with shock absorbing material," Proceedings of ROBOMEC '95 (Vol.A), 1995, pp.190-193 (in Japanese)

[15] Yoneda, K., "The development of a biped walking robot for HC-plane," 5th Conference of Robotics Society of Japan, 1987, pp.585-586 (in Japanese)

[16] Oh-hata, H., Yoneda, K., and Inoh, T., "Study of intelligent gait control of biped walking robot, — 1.Landing point adjustment using range finder," Proceedings of SICE'90, 1990, pp.229-230 (in Japanese)

[17] Zheng, Y.F. and Shen, J., "Gait Synthesis for the SD-2 Biped Robot to Climb Sloping Surface," IEEE Trans. on Robotics and Automation, Vol.6, No.1, 1990, pp.86-96